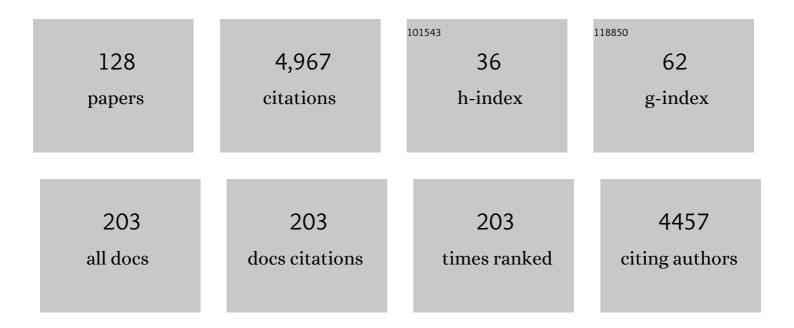


List of Publications by Year in descending order

Source: https://exaly.com/author-pdf/5629905/publications.pdf Version: 2024-02-01



رت⁰ رت∼√ مُ~

#	Article	IF	CITATIONS
1	Alkaliâ€Metalâ€Promoted Pt/TiO ₂ Opens a More Efficient Pathway to Formaldehyde Oxidation at Ambient Temperatures. Angewandte Chemie - International Edition, 2012, 51, 9628-9632.	13.8	611
2	Synergistic reaction between SO2 and NO2 on mineraloxides: a potential formation pathway of sulfate aerosol. Physical Chemistry Chemical Physics, 2012, 14, 1668-1676.	2.8	143
3	Degradation kinetics of levoglucosan initiated by hydroxyl radical under different environmental conditions. Atmospheric Environment, 2014, 91, 32-39.	4.1	129
4	Photocatalytic Removal of NO _{<i>x</i>} over Visible Light Responsive Oxygen-Deficient TiO ₂ . Journal of Physical Chemistry C, 2014, 118, 7434-7441.	3.1	116
5	Synergistic Effect between NO ₂ and SO ₂ in Their Adsorption and Reaction on γ-Alumina. Journal of Physical Chemistry A, 2008, 112, 6630-6635.	2.5	110
6	Heterogeneous OH Initiated Oxidation: A Possible Explanation for the Persistence of Organophosphate Flame Retardants in Air. Environmental Science & Technology, 2014, 48, 1041-1048.	10.0	102
7	Synergetic formation of secondary inorganic and organic aerosol: effect of SO ₂ and NH ₃ on particle formation and growth. Atmospheric Chemistry and Physics, 2016, 16, 14219-14230.	4.9	102
8	Influence of calcination temperature on iron titanate catalyst for the selective catalytic reduction of NOx with NH3. Catalysis Today, 2011, 164, 520-527.	4.4	98
9	Reactive uptake of ammonia to secondary organic aerosols: kinetics of organonitrogen formation. Atmospheric Chemistry and Physics, 2015, 15, 13569-13584.	4.9	90
10	Structural and hygroscopic changes of soot during heterogeneous reaction with O3. Physical Chemistry Chemical Physics, 2010, 12, 10896.	2.8	86
11	NO promotion of SO2 conversion to sulfate: An important mechanism for the occurrence of heavy haze during winter in Beijing. Environmental Pollution, 2018, 233, 662-669.	7.5	82
12	Seasonal Characteristics of New Particle Formation and Growth in Urban Beijing. Environmental Science & Technology, 2020, 54, 8547-8557.	10.0	78
13	Exploring the nitrous acid (HONO) formation mechanism in winter Beijing: direct emissions and heterogeneous production in urban and suburban areas. Faraday Discussions, 2016, 189, 213-230.	3.2	77
14	Ozone and SOA formation potential based on photochemical loss of VOCs during the Beijing summer. Environmental Pollution, 2021, 285, 117444.	7.5	75
15	Is reducing new particle formation a plausible solution to mitigate particulate air pollution in Beijing and other Chinese megacities?. Faraday Discussions, 2021, 226, 334-347.	3.2	74
16	Heterogeneous reaction of acetic acid on MgO, α-Al2O3, and CaCO3 and the effect on the hygroscopic behaviour of these particles. Physical Chemistry Chemical Physics, 2012, 14, 8403.	2.8	71
17	Role of Organic Carbon in Heterogeneous Reaction of NO ₂ with Soot. Environmental Science & Technology, 2013, 47, 3174-3181.	10.0	70
18	Sulfuric acid–amine nucleation in urban Beijing. Atmospheric Chemistry and Physics, 2021, 21, 2457-2468.	4.9	70

æ°_,æ~¥ Å~~

#	Article	IF	CITATIONS
19	Heterogeneous reaction of SO2 with soot: The roles of relative humidity and surface composition of soot in surface sulfate formation. Atmospheric Environment, 2017, 152, 465-476.	4.1	68
20	Key role of organic carbon in the sunlight-enhanced atmospheric aging of soot by O ₂ . Proceedings of the National Academy of Sciences of the United States of America, 2012, 109, 21250-21255.	7.1	66
21	Synergistic formation of sulfate and ammonium resulting from reaction between SO ₂ and NH ₃ on typical mineral dust. Physical Chemistry Chemical Physics, 2016, 18, 956-964.	2.8	66
22	In situ DRIFTS study of hygroscopic behavior of mineral aerosol. Journal of Environmental Sciences, 2010, 22, 555-560.	6.1	64
23	Secondary organic aerosol formed by condensing anthropogenic vapours over China's megacities. Nature Geoscience, 2022, 15, 255-261.	12.9	64
24	Heterogeneous Reaction of SO2 on Manganese Oxides: the Effect of Crystal Structure and Relative Humidity. Scientific Reports, 2017, 7, 4550.	3.3	56
25	Continuous and comprehensive atmospheric observations in Beijing: a station to understand the complex urban atmospheric environment. Big Earth Data, 2020, 4, 295-321.	4.4	54
26	The Synergistic Role of Sulfuric Acid, Bases, and Oxidized Organics Governing Newâ€Particle Formation in Beijing. Geophysical Research Letters, 2021, 48, e2020GL091944.	4.0	53
27	Significant source of secondary aerosol: formation from gasoline evaporative emissions in the presence of SO ₂ and NH ₃ . Atmospheric Chemistry and Physics, 2019, 19, 8063-8081.	4.9	52
28	Variation of size-segregated particle number concentrations in wintertime Beijing. Atmospheric Chemistry and Physics, 2020, 20, 1201-1216.	4.9	52
29	Heterogeneous photochemical aging of soot by NO2 under simulated sunlight. Atmospheric Environment, 2013, 64, 270-276.	4.1	50
30	Structure–activity relationship of surface hydroxyl groups during NO ₂ adsorption and transformation on TiO ₂ nanoparticles. Environmental Science: Nano, 2017, 4, 2388-2394.	4.3	49
31	Influence of Combustion Conditions on Hydrophilic Properties and Microstructure of Flame Soot. Journal of Physical Chemistry A, 2012, 116, 4129-4136.	2.5	46
32	A proxy for atmospheric daytime gaseous sulfuric acid concentration in urban Beijing. Atmospheric Chemistry and Physics, 2019, 19, 1971-1983.	4.9	46
33	A case study of Asian dust storm particles: Chemical composition, reactivity to SO2 and hygroscopic properties. Journal of Environmental Sciences, 2012, 24, 62-71.	6.1	43
34	Influence of relative humidity on heterogeneous kinetics of NO ₂ on kaolin and hematite. Physical Chemistry Chemical Physics, 2015, 17, 19424-19431.	2.8	43
35	Sources and sinks driving sulfuric acid concentrations in contrasting environments: implications on proxy calculations. Atmospheric Chemistry and Physics, 2020, 20, 11747-11766.	4.9	42
36	Comparisons of measured nitrous acid (HONO) concentrations in a pollution period at urban and suburban Beijing, in autumn of 2014. Science China Chemistry, 2015, 58, 1393-1402.	8.2	41

ư_,Æ~¥Å^~

#	Article	IF	CITATIONS
37	Chemical and Toxicological Evolution of Carbon Nanotubes During Atmospherically Relevant Aging Processes. Environmental Science & Technology, 2015, 49, 2806-2814.	10.0	37
38	The promotion effect of nitrous acid on aerosol formation in wintertime in Beijing: the possible contribution of traffic-related emissions. Atmospheric Chemistry and Physics, 2020, 20, 13023-13040.	4.9	37
39	Mechanism of Heterogeneous Reaction of Carbonyl Sulfide on Magnesium Oxide. Journal of Physical Chemistry A, 2007, 111, 4333-4339.	2.5	36
40	Degradation kinetics of anthracene by ozone on mineral oxides. Atmospheric Environment, 2010, 44, 4446-4453.	4.1	36
41	Review of heterogeneous photochemical reactions of NOy on aerosol — A possible daytime source of nitrous acid (HONO) in the atmosphere. Journal of Environmental Sciences, 2013, 25, 326-334.	6.1	36
42	Size-segregated particle number and mass concentrations from different emission sources in urban Beijing. Atmospheric Chemistry and Physics, 2020, 20, 12721-12740.	4.9	36
43	Heterogeneous reactivity of carbonyl sulfide on α-Al2O3 and γ-Al2O3. Atmospheric Environment, 2008, 42, 960-969.	4.1	35
44	Heterogeneous reactions between NO2 and anthracene adsorbed on SiO2 and MgO. Atmospheric Environment, 2011, 45, 917-924.	4.1	35
45	Effect of mineral dust on secondary organic aerosol yield and aerosol size in α-pinene/NOx photo-oxidation. Atmospheric Environment, 2013, 77, 781-789.	4.1	35
46	Heterogeneous Uptake of Amines by Citric Acid and Humic Acid. Environmental Science & Technology, 2012, 46, 11112-11118.	10.0	34
47	Unprecedented Ambient Sulfur Trioxide (SO ₃) Detection: Possible Formation Mechanism and Atmospheric Implications. Environmental Science and Technology Letters, 2020, 7, 809-818.	8.7	34
48	Acid–Base Clusters during Atmospheric New Particle Formation in Urban Beijing. Environmental Science & Technology, 2021, 55, 10994-11005.	10.0	34
49	Mesoporous transition alumina with uniform pore structure synthesized by alumisol spray pyrolysis. Chemical Engineering Journal, 2010, 163, 133-142.	12.7	33
50	Important role of aromatic hydrocarbons in SOA formation from unburned gasoline vapor. Atmospheric Environment, 2019, 201, 101-109.	4.1	33
51	Temperature Dependence of the Heterogeneous Reaction of Carbonyl Sulfide on Magnesium Oxide. Journal of Physical Chemistry A, 2008, 112, 2820-2826.	2.5	32
52	Experimental and Theoretical Study of Hydrogen Thiocarbonate for Heterogeneous Reaction of Carbonyl Sulfide on Magnesium Oxide. Journal of Physical Chemistry A, 2009, 113, 3387-3394.	2.5	32
53	Influence of functional groups on toxicity of carbon nanomaterials. Atmospheric Chemistry and Physics, 2019, 19, 8175-8187.	4.9	32
54	Contribution of Atmospheric Oxygenated Organic Compounds to Particle Growth in an Urban Environment. Environmental Science & Technology, 2021, 55, 13646-13656.	10.0	32

æ°_,æ~¥ Å~

#	Article	IF	CITATIONS
55	The Utilization of Physisorption Analyzer for Studying the Hygroscopic Properties of Atmospheric Relevant Particles. Journal of Physical Chemistry A, 2010, 114, 4232-4237.	2.5	30
56	Differences in the reactivity of ammonium salts with methylamine. Atmospheric Chemistry and Physics, 2012, 12, 4855-4865.	4.9	30
57	The effect of water on the heterogeneous reactions of SO ₂ and NH ₃ on the surfaces of α-Fe ₂ O ₃ and γ-Al ₂ O ₃ . Environmental Science: Nano, 2019, 6, 2749-2758.	4.3	30
58	Differences of the oxidation process and secondary organic aerosol formation at low and high precursor concentrations. Journal of Environmental Sciences, 2019, 79, 256-263.	6.1	29
59	Responses of gaseous sulfuric acid and particulate sulfate to reduced SO2 concentration: A perspective from long-term measurements in Beijing. Science of the Total Environment, 2020, 721, 137700.	8.0	28
60	Size-resolved particle number emissions in Beijing determined from measured particle size distributions. Atmospheric Chemistry and Physics, 2020, 20, 11329-11348.	4.9	28
61	Decreasing effect and mechanism of FeSO 4 seed particles on secondary organic aerosol in $\hat{l}\pm$ -pinene photooxidation. Environmental Pollution, 2014, 193, 88-93.	7.5	27
62	Secondary organic aerosol formation from the OH-initiated oxidation of guaiacol under different experimental conditions. Atmospheric Environment, 2019, 207, 30-37.	4.1	27
63	Influence of photochemical loss of volatile organic compounds on understanding ozone formation mechanism. Atmospheric Chemistry and Physics, 2022, 22, 4841-4851.	4.9	26
64	Effect of soot microstructure on its ozonization reactivity. Journal of Chemical Physics, 2012, 137, 084507.	3.0	25
65	Heterogeneous and multiphase formation pathways of gypsum in the atmosphere. Physical Chemistry Chemical Physics, 2013, 15, 19196.	2.8	25
66	Role of NH ₃ in the Heterogeneous Formation of Secondary Inorganic Aerosols on Mineral Oxides. Journal of Physical Chemistry A, 2018, 122, 6311-6320.	2.5	25
67	Ammonium nitrate promotes sulfate formation through uptake kinetic regime. Atmospheric Chemistry and Physics, 2021, 21, 13269-13286.	4.9	24
68	OH-initiated heterogeneous oxidation of tris-2-butoxyethyl phosphate: implications for its fate in the atmosphere. Atmospheric Chemistry and Physics, 2014, 14, 12195-12207.	4.9	23
69	The photoenhanced aging process of soot by the heterogeneous ozonization reaction. Physical Chemistry Chemical Physics, 2016, 18, 24401-24407.	2.8	23
70	A 3D study on the amplification of regional haze and particle growth by local emissions. Npj Climate and Atmospheric Science, 2021, 4, .	6.8	23
71	Amplified role of potential HONO sources in O ₃ formation in North China Plain during autumn haze aggravating processes. Atmospheric Chemistry and Physics, 2022, 22, 3275-3302.	4.9	23
72	Effects of Adding CeO2 to Ag/Al2O3 Catalyst for Ammonia Oxidation at Low Temperatures. Chinese Journal of Catalysis, 2011, 32, 727-735.	14.0	22

ư_,Æ~¥Å~~

#	Article	IF	CITATIONS
73	Heterogeneous Kinetics of <i>cis</i> -Pinonic Acid with Hydroxyl Radical under Different Environmental Conditions. Journal of Physical Chemistry A, 2015, 119, 6583-6593.	2.5	22
74	Enhancement of secondary organic aerosol formation and its oxidation state by SO ₂ during photooxidation of 2-methoxyphenol. Atmospheric Chemistry and Physics, 2019, 19, 2687-2700.	4.9	22
75	Effects of NO⁢sub>2⁢/sub> and C ₃ H ₆ on the heterogeneous oxidation of SO ₂ on TiO ₂ in the presence or absence of UV–Vis irradiation.	4.9	21
76	Atmospheric Chemistry and Physics, 2019, 19, 14777-14790. Particle growth with photochemical age from new particle formation to haze in the winter of Beijing, China. Science of the Total Environment, 2021, 753, 142207.	8.0	21
77	Application of smog chambers in atmospheric process studies. National Science Review, 2022, 9, nwab103.	9.5	21
78	Evolution of organic carbon during COVID-19 lockdown period: Possible contribution of nocturnal chemistry. Science of the Total Environment, 2022, 808, 152191.	8.0	21
79	Rate constant and secondary organic aerosol formation from the gas-phase reaction of eugenol with hydroxyl radicals. Atmospheric Chemistry and Physics, 2019, 19, 2001-2013.	4.9	20
80	Oxygen Poisoning Mechanism of Catalytic Hydrolysis of OCS over Al2O3 at Room Temperature. Acta Physico-chimica Sinica, 2007, 23, 997-1002.	0.6	19
81	An indicator for sulfuric acid–amine nucleation in atmospheric environments. Aerosol Science and Technology, 2021, 55, 1059-1069.	3.1	19
82	Insufficient Condensable Organic Vapors Lead to Slow Growth of New Particles in an Urban Environment. Environmental Science & Technology, 2022, 56, 9936-9946.	10.0	19
83	Ozonolysis of Trimethylamine Exchanged with Typical Ammonium Salts in the Particle Phase. Environmental Science & Technology, 2016, 50, 11076-11084.	10.0	18
84	Measurement report: Effects of photochemical aging on the formation and evolution of summertime secondary aerosol in Beijing. Atmospheric Chemistry and Physics, 2021, 21, 1341-1356.	4.9	18
85	Heterogeneous reactions of carbonyl sulfide on mineral oxides: mechanism and kinetics study. Atmospheric Chemistry and Physics, 2010, 10, 10335-10344.	4.9	17
86	Influence of sulfur in fuel on the properties of diffusion flame soot. Atmospheric Environment, 2016, 142, 383-392.	4.1	17
87	Influence of Chinese New Year overlapping COVID-19 lockdown on HONO sources in Shijiazhuang. Science of the Total Environment, 2020, 745, 141025.	8.0	17
88	Chemical characterization of submicron aerosol in summertime Beijing: A case study in southern suburbs in 2018. Chemosphere, 2020, 247, 125918.	8.2	17
89	Intelligent and Scalable Air Quality Monitoring With 5G Edge. IEEE Internet Computing, 2021, 25, 35-44.	3.3	17
90	Formation of nighttime sulfuric acid from the ozonolysis of alkenes in Beijing. Atmospheric Chemistry and Physics, 2021, 21, 5499-5511.	4.9	17

æ°,æ~¥ Å~

#	Article	IF	CITATIONS
91	Chemistry of new particle formation and growth events during wintertime in suburban area of Beijing: Insights from highly polluted atmosphere. Atmospheric Research, 2021, 255, 105553.	4.1	16
92	An interlaboratory comparison of aerosol inorganic ion measurements by ion chromatography: implications for aerosol pH estimate. Atmospheric Measurement Techniques, 2020, 13, 6325-6341.	3.1	16
93	Molecular Composition of Oxygenated Organic Molecules and Their Contributions to Organic Aerosol in Beijing. Environmental Science & amp; Technology, 2022, 56, 770-778.	10.0	16
94	Heterogeneous photochemical reaction of ozone with anthracene adsorbed on mineral dust. Atmospheric Environment, 2013, 72, 165-170.	4.1	15
95	Influence of metal-mediated aerosol-phase oxidation on secondary organic aerosol formation from the ozonolysis and OH-oxidation of α-pinene. Scientific Reports, 2017, 7, 40311.	3.3	15
96	Heterogeneous reaction of NO2 with soot at different relative humidity. Environmental Science and Pollution Research, 2017, 24, 21248-21255.	5.3	15
97	A large-scale outdoor atmospheric simulation smog chamber for studying atmospheric photochemical processes: Characterization and preliminary application. Journal of Environmental Sciences, 2021, 102, 185-197.	6.1	15
98	Laboratory study on OH-initiated degradation kinetics of dehydroabietic acid. Physical Chemistry Chemical Physics, 2015, 17, 10953-10962.	2.8	14
99	Secondary aerosol formation and oxidation capacity in photooxidation in the presence of Al2O3 seed particles and SO2. Science China Chemistry, 2015, 58, 1426-1434.	8.2	14
100	Identification, Quantification, and Imaging of the Biodistribution of Soot Particles by Mass Spectral Fingerprinting. Analytical Chemistry, 2021, 93, 6665-6672.	6.5	14
101	Heterogeneous oxidation of carbonyl sulfide on mineral oxides. Science Bulletin, 2007, 52, 2063-2071.	1.7	13
102	Heterogeneous uptake of carbonyl sulfide onto kaolinite within a temperature range of 220–330 K. Journal of Geophysical Research, 2010, 115, .	3.3	13
103	Distinct potential aerosol masses under different scenarios of transport at a suburban site of Beijing. Journal of Environmental Sciences, 2016, 39, 52-61.	6.1	13
104	Oxidation Potential Reduction of Carbon Nanomaterials during Atmospheric-Relevant Aging: Role of Surface Coating. Environmental Science & Technology, 2019, 53, 10454-10461.	10.0	13
105	Ozone formation sensitivity study using machine learning coupled with the reactivity of volatile organic compound species. Atmospheric Measurement Techniques, 2022, 15, 1511-1520.	3.1	13
106	Enhanced secondary organic aerosol formation from the photo-oxidation of mixed anthropogenic volatile organic compounds. Atmospheric Chemistry and Physics, 2021, 21, 7773-7789.	4.9	12
107	Atmospheric gaseous hydrochloric and hydrobromic acid in urban Beijing, China: detection, source identification and potential atmospheric impacts. Atmospheric Chemistry and Physics, 2021, 21, 11437-11452.	4.9	12
108	Technical Note: Application of positive matrix factor analysis in heterogeneous kinetics studies utilizing the mixed-phase relative rates technique. Atmospheric Chemistry and Physics, 2014, 14, 9201-9211.	4.9	11

ư_,Æ~¥Å~~

#	Article	IF	CITATIONS
109	Stability of polycyclic aromatic compounds in polyurethane foam-type passive air samplers upon O3 exposure. Atmospheric Environment, 2015, 120, 200-204.	4.1	11
110	Ageing remarkably alters the toxicity of carbon black particles towards susceptible cells: determined by differential changes of surface oxygen groups. Environmental Science: Nano, 2020, 7, 1633-1641.	4.3	11
111	Assessment of particle size magnifier inversion methods to obtain the particle size distribution from atmospheric measurements. Atmospheric Measurement Techniques, 2020, 13, 4885-4898.	3.1	11
112	Rapid mass growth and enhanced light extinction of atmospheric aerosols during the heating season haze episodes in Beijing revealed by aerosol–chemistry–radiation–boundary layer interaction. Atmospheric Chemistry and Physics, 2021, 21, 12173-12187.	4.9	10
113	A direct sulfation method for introducing the transition metal cation Co2+ into ZrO2 with little change in the BrĀ,nsted acid sites. Journal of Catalysis, 2011, 279, 301-309.	6.2	8
114	Effect of aluminium dust on secondary organic aerosol formation in m-xylene/NO x photo-oxidation. Science China Earth Sciences, 2015, 58, 245-254.	5.2	8
115	Influence of organic aerosol molecular composition on particle absorptive properties in autumn Beijing. Atmospheric Chemistry and Physics, 2022, 22, 1251-1269.	4.9	8
116	Nontarget Screening Exhibits a Seasonal Cycle of PM _{2.5} Organic Aerosol Composition in Beijing. Environmental Science & Technology, 2022, 56, 7017-7028.	10.0	8
117	Effects of ultrasonic treatment on dithiothreitol (DTT) assay measurements for carbon materials. Journal of Environmental Sciences, 2019, 84, 51-58.	6.1	7
118	A New Type of Quartz Smog Chamber: Design and Characterization. Environmental Science & Technology, 2022, 56, 2181-2190.	10.0	7
119	Measurement report: New particle formation characteristics at an urban and a mountain station in northern China. Atmospheric Chemistry and Physics, 2021, 21, 17885-17906.	4.9	7
120	Alumina with Various Pore Structures Prepared by Spray Pyrolysis of Inorganic Aluminum Precursors. Industrial & Engineering Chemistry Research, 2013, 52, 13377-13383.	3.7	6
121	N-nitration of secondary aliphatic amines in the particle phase. Chemosphere, 2022, 293, 133639.	8.2	6
122	Influence of Aerosol Chemical Composition on Condensation Sink Efficiency and New Particle Formation in Beijing. Environmental Science and Technology Letters, 2022, 9, 375-382.	8.7	6
123	Long-term winter observation of nitrous acid in the urban area of Beijing. Journal of Environmental Sciences, 2022, 114, 334-342.	6.1	5
124	Highly oxidized organic aerosols in Beijing: Possible contribution of aqueous-phase chemistry. Atmospheric Environment, 2022, 273, 118971.	4.1	3
125	Ageing Significantly Alters the Physicochemical Properties and Associated Cytotoxicity Profiles of Ultrafine Particulate Matters towards Macrophages. Antioxidants, 2022, 11, 754.	5.1	3
126	The impact of ammonium on the distillation of organic carbon in PM2.5. Science of the Total Environment, 2022, 803, 150012.	8.0	2

æ°,æ~¥ Å~

#	Article	IF	CITATIONS
127	Retrieval of Multiple Atmospheric Environmental Parameters From Images With Deep Learning. IEEE Geoscience and Remote Sensing Letters, 2022, 19, 1-5.	3.1	2
128	Heterogeneous kinetics of the OH-initiated degradation of fenthion and parathion. Journal of Environmental Sciences, 2023, 133, 161-170.	6.1	1